Analyst

Cite this: *Analyst*, 2011, **136**, 4682

www.rsc.org/analyst

PAPER

Determination of morphine at gold nanoparticles/Nafion® carbon paste modified sensor electrode†‡§

Nada F. Atta,* Ahmed Galal and Shereen M. Azab

Received 24th May 2011, Accepted 26th July 2011
DOI: 10.1039/c1an15423k

A novel and effective electrochemical sensor for the determination of morphine (MO) in 0.04 mol L^{-1} universal buffer solution (pH 7.4) is introduced using gold nanoparticles electrodeposited on a Nafion modified carbon paste electrode. The effect of various experimental parameters including pH, scan rate and accumulation time on the voltammetric response of MO was investigated. At the optimum conditions, the concentration of MO was determined using differential pulse voltammetry (DPV) in a linear range of 2.0×10^{-7} to 2.6×10^{-4} mol L^{-1} with a correlation coefficient of 0.999, and a detection limit of 13.3×10^{-10} mol L^{-1}, respectively. The effect of common interferences on the current response of morphine namely ascorbic acid (AA) and uric acid (UA) is studied. The modified electrode can be used for the determination of MO spiked into urine samples, and excellent recovery results were obtained.

1. Introduction

Morphine (MO), a phenolic compound and an alkaloid which can cause disruption in the central nervous system, is frequently used to relieve severe pain in patients, especially those undergoing a surgical procedure.

Morphine (Fig. S1§) was the first active principle ingredient purified from a plant source and is one of at least 50 alkaloids of several different types present in opium, Poppy Straw and other poppy derivatives.

In clinical medicine, morphine is regarded as the gold standard, or the benchmark, of analgesics used to relieve severe or agonizing pain and suffering. Like other opioids morphine acts directly on the central nervous system (CNS) to relieve pain. Morphine has a high potential for addiction; tolerance and psychological dependence develop rapidly.

Nafion is a perfluorinated sulfonated cation exchanger and consists of a linear backbone of fluorocarbon chains and ethyl ether pendant groups with sulfonic cation exchange sites (Fig. S2§). The increasing popularity of Nafion for the fabrication of modified electrodes in recent years arises from easy fabrication, good electrical conductivity and high partition coefficients of many redox compounds in Nafion.[1] Nafion has been often used in the modification of carbon paste electrode (CPE),[2,3] glassy carbon electrodes,[4] carbon fiber microelectrodes[5] and mercury film electrodes.[6–8] A very thin film of Nafion is ample to offer minimal obstruction to the diffusion of the analyte to the electrode, while preventing at the same time adsorption–desorption processes of organic species in biological fluids.[9] Some authors incorporate the Nafion into the carbon paste during the mixing of the graphite and Nujol.[10] Others applied the Nafion polymer layer on top of the surface of the CPE.[3] One important reason for the widespread application of Nafion modified electrodes in electroanalytical chemistry is their ability to preconcentrate positively charged molecules which increase the sensitivity of the method.[11–15] The accumulation mechanism of Nafion can be explained through an electrostatic interaction due to the hydrophilic negatively charged sulfonate groups in the polymer structure, whereas its ionic selectivity for hydrophobic organic cations is achieved through hydrophobic interactions with the hydrophobic fluorocarbons of the film.[16]

Gold nanoparticles (GNPs), with large surface area, good biocompatibility, high conductivity and electrocatalysis characteristics, have been used to improve the detection limits in electrochemical studies.[17–23] They are also suitable for many surface immobilization mechanisms and can act as tiny conduction centers and can facilitate the transfer of electrons.

To date various analytical methods have been developed for the determination of morphine including gas chromatography,[24,25] high-performance liquid chromatography (HPLC)[26–31] and their combination with other detection methods. Immunoassays such

Department of Chemistry, Faculty of Science, Cairo University, Giza, 12613, Egypt. E-mail: nada_fah1@yahoo.com; Fax: +20 02 35727556; Tel: +20 02 35676561

† This article is part of a web theme in *Analyst* and *Analytical Methods* on Future Electroanalytical Developments, highlighting important developments and novel applications. Also in this theme is work presented at the Eirelec 2011 meeting, dedicated to Professor Malcolm Smyth on the occasion of his 60th birthday.

‡ The authors would like to dedicate this work to Prof. Malcolm R. Smyth on the occasion of his 60th birthday in recognition to his invaluable contribution in the areas of modified electrodes and biosensors.

§ Electronic supplementary information (ESI) available. See DOI: 10.1039/c1an15423k

as surface plasmon resonance (SPR) based immunosensors[32,33] and radioimmunoassays (RIA)[34] are also reported for morphine detection. The use of bare electrodes such as platinum electrode,[35] glassy carbon electrode and graphite electrode[36] has proved to be straightforward and simple in detecting morphine. Compared to other methods, electroanalysis has the advantages of simplicity and high sensitivity. However the use of bare electrodes for electrochemical measurements has a number of limitations, such as slow electron transfer reaction and electrode fouling problems. Recently, some new electrochemical detection methods have been proposed for morphine detection. For example, an adsorptive differential pulse stripping method[37] and its conjugation with least squares support vector machines[38] have been developed for trace morphine detection. Fast Fourier transformation with continuous cyclic voltammetry at Au microelectrode[39,40] has been devised for morphine detection in a flow injection system. Furthermore, different modified electrodes have been developed for morphine detection. For example, Jin and co-workers prepared a kind of cobalt hexacyanoferrate modified carbon paste electrode, combined it with HPLC and successfully detected morphine *in vivo*.[41] Ho *et al.* devised a Prussian blue-modified indium tin oxide (ITO) electrode[42] and molecularly imprinted electrodes for morphine determination.[43,44] A multiwalled carbon nanotube modified preheated glassy carbon electrode has also been used for the morphine detection.[45] A Prussian blue film modified-palladized aluminium electrode[46] has recently been used for morphine detection.

The aim of this study is to construct a novel, stable and sensitive electrochemical sensor based on gold nanoparticles, Nafion and graphite, to be used for the determination of morphine. The electrochemical behaviors of morphine at our modified electrode will be investigated using CV and differential pulse voltammetry (DPV) techniques. The detection of MO in the tablet sample and human urine will be demonstrated as real sample applications.

2. Experimental

2.1. Materials and reagents

Morphine sulfate was used as received. A 10% Nafion solution purchased from Aldrich (dissolved in a lower aliphatic alcohol and water) was immobilized in the matrix of CPE. Britton–Robinson (B–R) (4.0×10^{-2} mol L^{-1}) buffer solution of pH 2–11 (CH_3COOH + H_3BO_3 + H_3PO_4) was used as the supporting electrolyte. The pH was adjusted using 0.2 mol L^{-1} NaOH. All solutions were prepared from analytical grade chemicals and sterilized Milli-Q deionized water.

2.1.1. Construction of the modified carbon-paste electrodes. The unmodified carbon-paste electrode (UCPE) was prepared by mixing graphite powder with an appropriate amount of mineral oil (nujol) and thorough hand mixing in a mortar and pestle (75 : 25, w/w, %). A portion of the composite mixture was packed into the end of the CPE. To prepare the Nafion-incorporated carbon paste electrode (NCPE) [electrode (1)], a mixture of Nafion solution, nujol and graphite powder (10 : 15 : 75, w/w, %) with a total weight of 1.00 g was transferred to the mortar and pestle and then homogenized by adding 2.0 ml of dichloromethane. The solvent was evaporated at room temperature (for 24 h) and the resulting composite was packed in the electrode.[47]

To construct the GNPs modified NCPE [electrode (2)], [electrode (1)] was immersed into 6 mmol L^{-1} of hydrogen-tetrachloroaurate $HAuCl_4$ solution containing 0.1 mol L^{-1} KNO_3 (prepared in doubly distilled water, and deaerated by bubbling with nitrogen). A constant potential of −0.4 V *versus* Ag/AgCl was applied for 400 s. Then, the modified electrode was washed with doubly distilled water and dried carefully.

2.2. Instrumental and experimental setup

2.2.1. Electrochemical measurements. All voltammetric measurements were performed using a pc-controlled AEW2 electrochemistry workstation and data were analyzed with EC_{prog3} electrochemistry software, manufactured by SYCOPEL SCIENTIFIC LIMITED (Tyne & Wear, UK). The one compartment cell with the three electrodes was connected to the electrochemical workstation through a C_3-stand from BAS (USA). A platinum wire from BAS (USA) was employed as an auxiliary electrode. All the cell potentials were measured with respect to the Ag/AgCl (3 mol L^{-1} NaCl) reference electrode from BAS (USA). The one compartment glass cell (15 ml) fitted with a gas bubbler was used for electrochemical measurements. Solutions were degassed using pure nitrogen prior and throughout the electrochemical measurements. A JENWAY 3510 pH meter (England) with a glass combination electrode was used for pH measurements. Scanning electron microscopy (SEM) measurements were carried out using a JSM-6700F scanning electron microscope (Japan Electro Company). All the electrochemical experiments were performed at an ambient temperature of 25 ± 2 °C.

2.2.2. Impedance spectroscopy measurements. Electrochemical impedance spectroscopy was performed using a Gamry-750 system and a lock-in-amplifier that are connected to a personal computer. The data analysis software was provided with the instrument and applied non-linear least square fitting with the Levenberg–Marquardt algorithm. The parameters in an electrochemical impedance experiment were as follows: different potential values 0.43 V and 0.25 V studied at a frequency range of 0.1–10 000 Hz with an amplitude of 5 mV were applied on [electrode (1)] and [electrode (2)] which were tested in 1.0 mmol L^{-1} MO.

2.3. Analysis of urine

Standard MO provided by the National Organization for Drug Control and Research of Egypt was dissolved in urine to make a stock solution with 1.0×10^{-3} mol L^{-1} concentration. Successive additions of 1.0×10^{-3} mol L^{-1} MO in urine were added to 5 ml B–R buffer, pH 7.4.

3. Results and discussion

3.1. Morphologies of the different electrodes

The response of an electrochemical sensor was related to its physical morphology. The SEM of [electrode (1)] and [electrode

(2)] is shown in Fig. 1. Significant differences in the surface structure of [electrode (1)] and [electrode (2)] were observed. The surface of [electrode (1)] was predominated by isolated and irregularly shaped graphite flakes and separated layers were noticed (Fig. 1A). The SEM image of [electrode (2)] (Fig. 1B) shows that metallic nanoparticles are located at different elevations over the substrate. Moreover, a random distribution and interstices among the nanoparticles were observed in the SEM image of [electrode (2)] exhibiting a large surface area.

3.2. Electrochemistry of MO at GNPs modified NCPE

The voltammetric behavior of MO was examined using cyclic voltammetry. Fig. 2 shows typical cyclic voltammograms of 1.0×10^{-3} mol L^{-1} of morphine (MO) in B–R buffer, pH 7.4, at a scan rate of 100 mV s^{-1} recorded at two different working electrodes (*i.e.* [electrode (1)] (solid lines) and [electrode (2)] (dashed lines)). For [electrode (1)] an anodic peak current of 30.8 μA was observed at +0.484 V while for [electrode (2)] the anodic peak current was 84.14 at +0.433 V which was produced due to the oxidation of the phenolic group at the 3-position of morphine, which involves one electron transfer. The oxidation of the phenolic group leads to the formation of pseudomorphine (PM) as the main product. Since the structure of pseudomorphine possesses two phenolic groups it makes its further oxidation possible.[35] However, the oxidation occurs at the same potential as morphine.[48] Therefore, the peak at +0.433 V is ascribed to oxidation of the phenolic groups in morphine and pseudomorphine (eqn (1)–(5)).

$$\text{M–OH (morphine)} \leftrightarrow \text{M–O}^- + \text{H}^+ \quad (1)$$

$$\text{M–O}^- \leftrightarrow \text{M–O*} + \text{e}^- \quad (2)$$

$$2\text{M–O*} \leftrightarrow \text{PM–OH} \quad (3)$$

$$\text{PM–OH} \leftrightarrow \text{PM–O}^- + \text{H}^+ \quad (4)$$

$$\text{PMO}^- \leftrightarrow \text{PM–O*} + \text{e}^- \quad (5)$$

The electrodeposition of GNPs on [electrode (1)] resulted in an observable increase in the peak current, which indicated an improvement in the electrode kinetics and a decrease in the potential of oxidation substantially (*i.e.* thermodynamically feasible reaction). This is due to the larger surface area of the

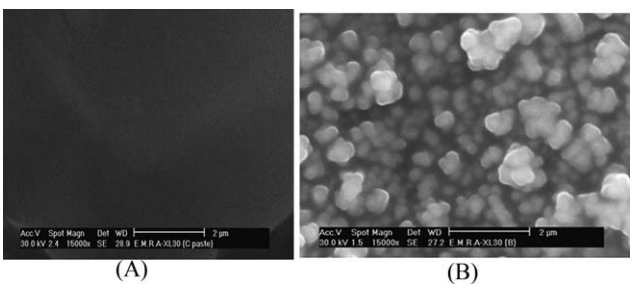

Fig. 1 (A) The scanning electron microscope image of [electrode (1)]. (B) The scanning electron microscope image of [electrode (2)].

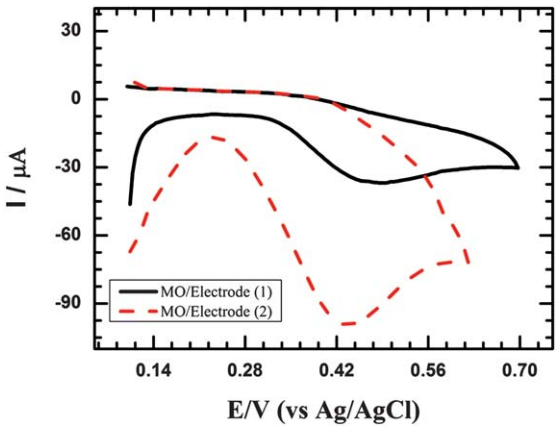

Fig. 2 Cyclic voltammograms of 1.0×10^{-3} mol L^{-1} MO in B–R buffer, pH 7.4, at a scan rate of 100 mV s^{-1} recorded at two different working electrodes [electrode (1)] (—) and [electrode (2)] (---).

modified electrode and the synergism effect of the electronic conductivity and electroactivity of gold metallic properties with ionic conductivity and ion-exchange capacity of Nafion. The results confirmed the key role played by GNPs and Nafion in the catalytic oxidation which enhances the electrochemical reaction.

3.3. Effect of operational parameters

3.3.1. Effect of solution pH. The effect of solution pH on the electrocatalytic oxidation of MO at [electrode (2)] was studied by the cyclic voltammogram technique using Britton–Robinson buffers in the pH range of 2–10 (Fig. 3). The insets show the comparison between the anodic peak currents and potentials at different pH values of [electrode (1)] and [electrode (2)], which show that the pH of the solution has a significant influence on the oxidation peak potential of MO, *i.e.* the anodic peak potentials shifted negatively with the increase of the solution pH, indicating that the electrocatalytic oxidation at [electrode (2)] is

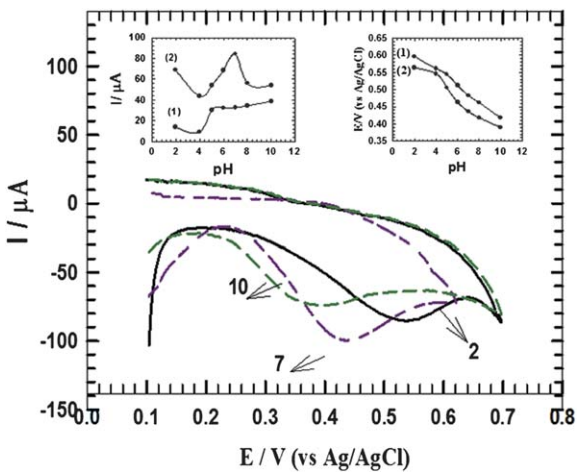

Fig. 3 Cyclic voltammograms of the effect of solution pH on the electrocatalytic oxidation of MO at [electrode (2)] using Britton–Robinson buffers in the pH 2, 7, and 10. Insets: comparison between the anodic peak currents and potentials at different pH values of [electrode (1)] and [electrode (2)].

a pH-dependent reaction and that protons have taken part in their electrode reaction processes. Also, the peak potential for MO oxidation varies linearly with pH (over the pH range from 2 to 10). As the MO oxidation is a one-electron process, the number of protons involved was also predicted to be one indicating a $1e^-/1H^+$ process.

Also the comparison between the anodic peak currents at different pH values of [electrode (1)] and [electrode (2)] showed that by using [electrode (2)] the MO's anodic current responses decreased from pH 2 to pH 4, then increased to reach its highest value at pH 7 and then decreased slightly to reach nearly equal values at pH 8 and pH 10. It is clear that at high pH values the current responses were higher than those at low pH values, this is due to the pK_a value of MO which is 8.08,[49] therefore, the protonated morphine can be attracted by the negative charge of gold nanoparticles, which indicates the effect of gold nanoparticles on the catalytic oxidation processes.

3.3.2. Effect of scan rate. The effect of different scan rates (ν ranging from 10 to 250 mV s^{-1}) on the current response of MO (1.0×10^{-3} mol L^{-1}) on [electrode (2)] in B–R buffer (pH 7.4) was studied and a plot of i_{pa} *versus* $\nu^{1/2}$ gave a straight line relationship (Fig. 4). This revealed that the linearity of the relationship was realized up to a scan rate of 250 mV s^{-1}.

This indicated that the charge transfer was under diffusion control. A good linear relationship was found for the oxidation peak currents and potentials at different scan rates. The oxidation peak currents increased linearly with the linear regression equations as i_{pa} (10^{-6} A) $= -13.58\,\nu^{1/2}$ (V $s^{-1})^{1/2} - 8.57$ ($n = 7$, $\gamma = 0.9938$), suggesting that the reaction is a diffusion-controlled electrode reaction. Typical CV curves of MO at different scan rates are shown in the inset of Fig. 4. The other inset shows that the peak potential also increased with the scan rate.

The dependence of the anodic peak current density on the scan rate has been used for the estimation of the "apparent" diffusion coefficient, D_{app}, for the compounds studied. D_{app} values were calculated from the Randles Sevcik equation[50]

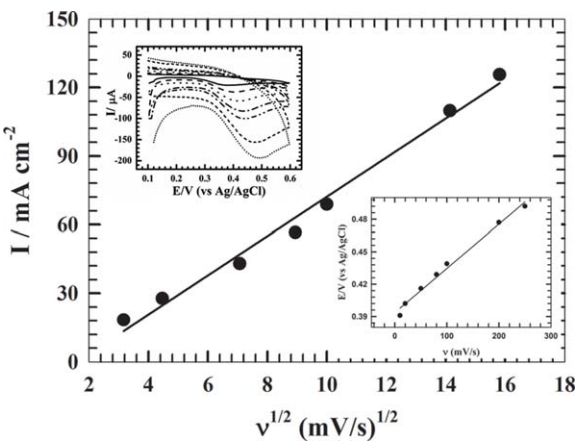

Fig. 4 Plot of the anodic peak current values *versus* square root of the scan rate. 1st inset: cyclic voltammograms of 1.0×10^{-3} mol L^{-1} MO at [electrode (2)] in the 0.04 M B–R buffer, pH 7.4, at: 10, 25, 50, 80, 100, 200 and 250 mV s^{-1}. 2nd inset: plot of the anodic peak potential values *versus* the scan rate.

$$i_{pa} = (2.69 \times 10^5) n^{3/2} A C_0^* D_0^{1/2} \nu^{1/2}$$

where the constant has units (*i.e.* 2.687×10^5 C mol^{-1} $V^{-1/2}$).

In these equations: i_p is the peak current density (A cm^{-2}), n is the number of electrons appearing in half-reaction for the redox couple, ν is the rate at which the potential is swept (V s^{-1}), F is Faraday's constant (96 485C mol^{-1}), C_0 is the analyte concentration (1×10^{-6} mol cm^{-3}), A is the electrode area (0.0706 cm^2), and D is the electroactive species diffusion coefficient (cm^2 s^{-1}). The apparent surface area used in the calculations did not take into account the surface roughness.

The apparent diffusion coefficients, D_{app}, of MO on [electrode (2)] in B–R buffer (pH 7.4) were calculated from cyclic voltammetry (CV) experiments and were found to be 2.69×10^{-6} cm^2 s^{-1}; this result was compared to that in the case of [electrode (1)] which is 5.25×10^{-7} cm^2 s^{-1}. This indicates the quick mass transfer of the analyte molecules towards the [electrode (2)] surface from bulk solutions and/or a fast electron transfer process of electrochemical oxidation of the analyte molecule at the electrode–solution interface.[51,52] Furthermore, it also showed that the redox reaction of the analyte species takes place at the surface of the electrode under the control of the diffusion of the molecules from solution to the electrode surface.

3.4. Electrochemical impedance spectroscopy (EIS) studies

EIS is an effective tool for studying the interface properties of surface modified electrodes. EIS data were obtained for [electrode (2)] at ac frequency varying between 0.1 Hz and 100 kHz with an applied potential in the region corresponding to the electrolytic oxidation of MO in B–R buffer, pH 7.4. Fig. 5A shows a typical impedance spectrum presented in the form of a Nyquist plot of MO using the (a) bare CP electrode, (b) [electrode (1)] and (c) [electrode (2)] at the oxidation potential of 430 mV. From this comparison, it is clear that the impedance responses of MO show a great difference in the presence of Nafion and gold nanoparticles.

It is clear that the impedance responses of MO show a great difference between the three cases, *i.e.* in the case of the bare CP electrode, the impedance spectra of MO include a semicircle with a larger diameter than in the case of [electrode (1)], where after deposition of gold [electrode (2)], the diameter of the semicircle diminishes markedly and the charge transfer resistance of electrooxidation of MO decreases greatly, and the charge transfer rate is enhanced. To obtain the detailed information of the impedance spectroscopy, a simple equivalent circuit model shown in Fig. 5B was used to fit the results.

The experimental data were compared to an "equivalent circuit". In this circuit, R_u is the solution resistance, R_p is the charge transfer resistance, CPE represents the predominant diffusion influence on the charge transfer, n is its corresponding exponent, C_f is the capacitance of the double layer and W is the Warburg impedance due to diffusion. Table 1 lists the best fitting values calculated from the equivalent circuit for the impedance data at 250 mV and 430 mV for each electrode. From the data indicated in Table 1, the value of solution resistance, R_u, was almost constant within the limits of the experimental errors. On the other hand, the electronic charge transfer resistance, R_p, shows a noticeable decrease in values in the case of [electrode (2)]

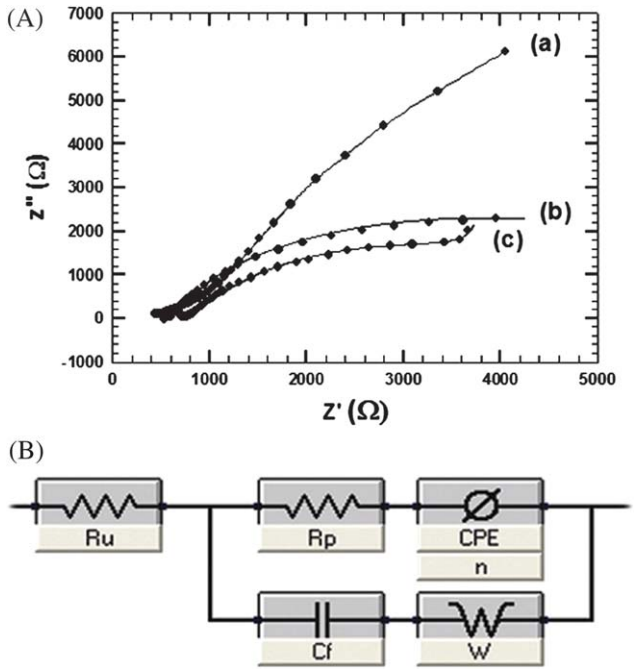

Fig. 5 (A) The typical impedance spectrum presented in the form of a Nyquist plot of MO using the (a) bare CP electrode, (b) [electrode (1)] and (c) [electrode (2)] at the oxidation potential of 430 mV. (Symbols and solid lines represent the experimental measurements and the computer fitting of impedance spectra, respectively.). (B) Equivalent circuit used in the fit procedure of the impedance spectra.

compared to [electrode (1)] and also in the case of [electrode (1)] compared to the bare CP electrode, which indicates less electronic resistance and more facilitation of charge transfer of [electrode (2)] > [electrode (1)] > bare CP electrode. The capacitive component value of [electrode (2)] is relatively higher compared to those of [electrode (1)] and bare CP electrode. This is explained in terms of the increase in the ionic adsorption at the electrode/electrolyte interface. Moreover, the decrease in the interfacial electron transfer resistance is attributed to the selective interaction between gold nanoparticles and MO that resulted in the observed increase in the current signal for the electro-oxidation process.

3.5. The effect of accumulation time on the response of MO

The effect of accumulation time on the oxidation peak current of morphine was examined using the cyclic voltammetry mode (Fig. 6). The resulting oxidation current *versus* time plot is displayed in the inset of Fig. 6, which indicated that the oxidation

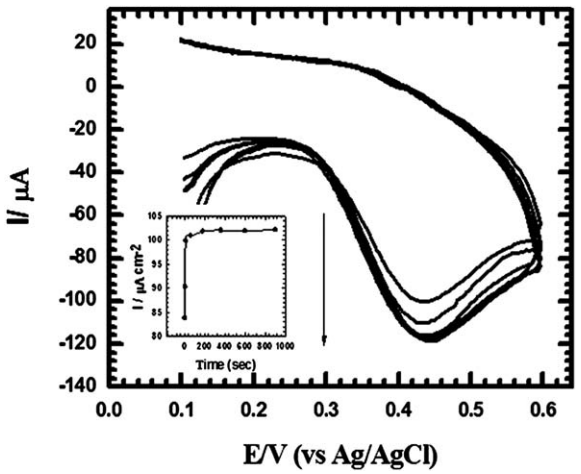

Fig. 6 Cyclic voltammogram of the effect of accumulation time on the oxidation peak current of 1.0×10^{-3} mol L^{-1} MO at [electrode (2)] in the 0.04 M B–R buffer pH 7.4.

peak current of morphine increased rapidly with the accumulation time at the first 10 seconds and then stayed stable up to 15 minutes. Thus accumulation time of 10 seconds under open-circuit conditions was employed.

3.6. Calibration curve

The calibration curves were constructed as aliquots of the drug solution (1.0×10^{-3} mol L^{-1}) were introduced into the electrolytic cell and voltammetric analyses were carried out and the voltammograms were recorded. The peak current was evaluated as the difference between each voltammogram and the background electrolyte voltammogram. Pulse voltammetric techniques such as DPV are effective and rapid electroanalytical techniques with well-established advantages, including good discrimination against background current and low detection limits. To prove the sensitivity of [electrode (2)] towards the electrochemical measurement of MO, the effect of changing the concentration of MO in B–R buffer, pH 7.4, using the DPV mode was studied (Fig. 7). The following are the parameters for the DPV experiment: $E_i = 100$ mV, $E_f = 600$ mV, scan rate = 10 mV s^{-1}, pulse width = 25 ms, pulse period = 200 ms, and pulse amplitude = 10 mV. The corresponding calibration plot is given in the inset. The calibration plot was linearly related to the MO concentration over the ranges of 2.0×10^{-7} to 2.6×10^{-4} mol L^{-1} with the regression equation of I_p (μA) = 0.029*c* (μM) + 0.891 and the correlation coefficient was 0.999. The limits of detection (LOD) and the limits of quantitation (LOQ) were calculated

Table 1 Electrochemical impedance spectroscopy fitting data corresponding to Fig. 5A

Electrode	*E*/mV	R_p/kΩ cm²	R_u/kΩ cm²	C_f/μF cm^{-2}	*W*/kΩ^{-1} cm^{-2}	CPE/μF cm^{-2}	*n*
CP electrode	250	182	0.49	0.31	40.07	8.05	0.34
	430	120	0.46	0.91	35.00	11.00	0.49
Electrode (1)	250	74.7	0.55	4.18	17.64	11.8	0.65
	430	30.0	0.56	7.49	10.84	14.7	0.55
Electrode (2)	250	10.3	0.47	9.51	2.16	26.9	0.71
	430	3.81	0.44	11.14	1.15	28.1	0.62

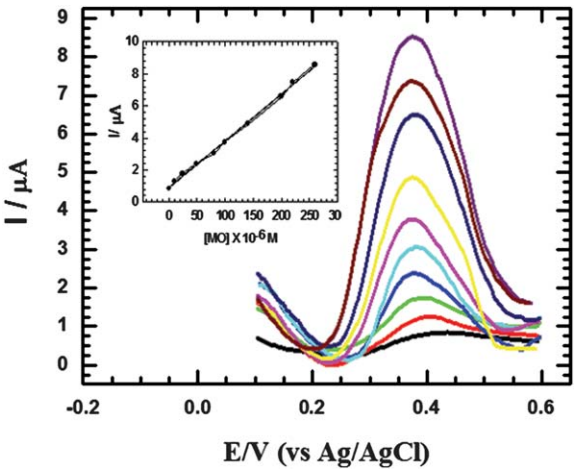

Fig. 7 The effect of changing the concentration of MO, using differential pulse modes at [electrode (2)] in the 0.04 M B–R buffer, pH 7.4, and a scan rate of 10 mV s^{-1}. The inset: the relation between different MO concentrations and the current responses.

from the oxidation peak currents of the two linear ranges using the following equations:

$$\mathrm{LOD} = 3s/m$$

$$\mathrm{LOQ} = 10s/m$$

where s is the standard deviation of the oxidation peak current (three runs) and m is the slope (μA mol^{-1} L) of the related calibration curves, and they were found to be 13.3×10^{-10} mol L^{-1} and 4.44×10^{-9} mol L^{-1} respectively. Both LOD and LOQ values confirmed the sensitivity of [electrode (2)]. Comparison of the detection limit and the sensitivity of MO by the proposed method with other reported methods in the literature is illustrated in Table 2.

4. Action of morphine on biological compounds

4.1. Morphine and neurotransmitters

The increase of plasma catecholamines that occurs during surgery can be reduced by administration of morphine. This is due to the fact that morphine specifically blocks nociceptive stimulation during surgery. The mechanism of action of morphine may have its etiology in concurrent modulation of more than one neurotransmitter. Moreover, in invertebrates, dopamine (DA) acts as the major molecule used in neural systems. In vertebrates, epinephrine emerges as the major end of the catecholamines. Fig. 8A shows the voltammetric response at [electrode (2)], in 0.1 mmol L^{-1} MO solution containing 0.1 mM DA in B–R buffer (pH 7.4). DA usually interferes with MO analysis in urine and blood. [Electrode (2)] gives two well defined oxidation peaks at +0.179 V and +0.398 V for DA and MO,

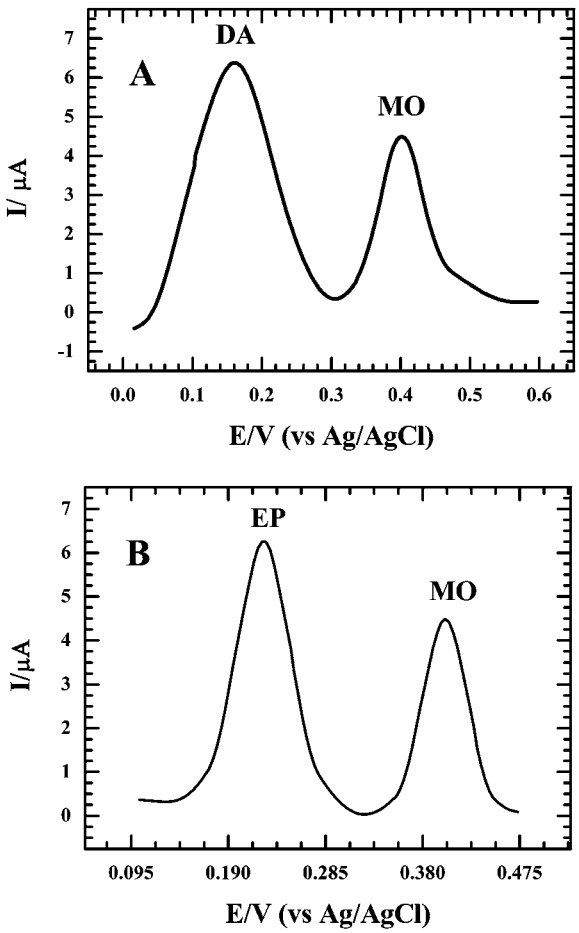

Fig. 8 (A) The differential pulse voltammetric response at [electrode (2)], in 0.1 mmol L^{-1} MO solution containing 0.1 mmol L^{-1} DA in B–R buffer (pH 7.4). (B) The differential pulse voltammetric response at [electrode (2)], in 0.1 mmol L^{-1} MO solution containing 0.1 mmol L^{-1} EP in B–R buffer (pH 7.4).

Table 2 Comparison of [electrode (1)] with the reported methods for the determination of MO

Detection method	Detection limit	Reference
LPME[a]-HPLC[b]	0.18 μmol L^{-1}	Zhang *et al.* (2008)
Microchip capillary electrophoresis	0.20 μmol L^{-1}	Zhang *et al.* (2007)
Sequential injection analysis	0.27 μmol L^{-1}	Idris and Alnajjar (2008)
Differential pulse voltammetry	0.01 μmol L^{-1}	Niazi *et al.* (2007)
Amperometry	0.20 μmol L^{-1}	Zhao *et al.* (2009)
Voltammetry	0.01 μmol L^{-1}	Fei Li *et al.* (2010)
Proposed method	1.33 nmol L^{-1}	This work

[a] Liquid phase micro-extraction [b] High performance Liquid chromatography

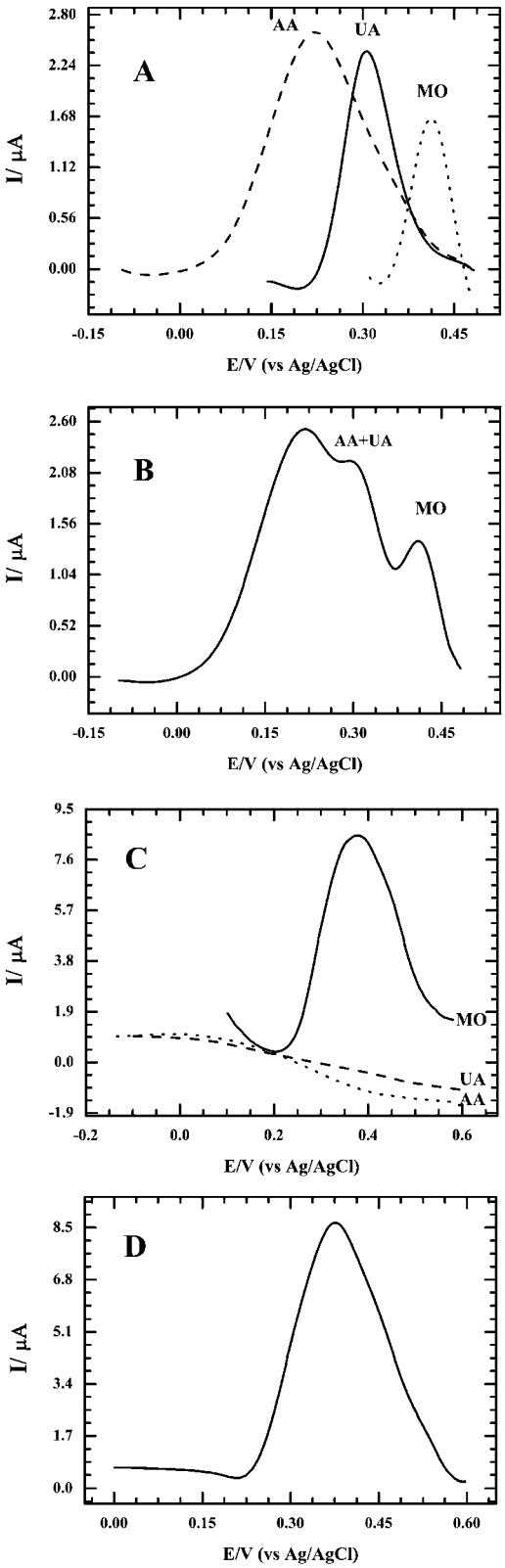

Fig. 9 (A) The differential pulse curves of 5.0 mmol L^{-1} AA, 1.0 mmol L^{-1} UA and 0.5 mmol L^{-1} MO measured separately, using [electrode (1)]. (B) The differential pulse curve of a mixture of 5.0 mmol L^{-1} AA, 1.0 mmol L^{-1} UA and 0.5 mmol L^{-1} MO, all in the same solution, using [electrode (1)]. (C) The differential pulse curves of 5.0 mmol L^{-1} AA, 1.0 mmol L^{-1} UA and 0.5 mmol L^{-1} MO measured separately, using [electrode (2)]. (D) The differential pulse curve of a mixture of 5.0 mmol L^{-1} AA, 1.0 mmol L^{-1} UA and 0.5 mmol L^{-1} MO, all in the same solution, using [electrode (2)].

respectively. This illustrates that it is possible to discriminate morphine from dopamine with good separation in the peak potential (ΔE = +0.22 V) and with relatively high oxidation current values.

Morphine withdrawal increases the turnover of epinephrine in the heart so studying both compounds in the presence of each other is necessary. The DPV technique (Fig. 8B) shows the voltammetric response at [electrode (2)], in 0.1 mmol L^{-1} MO solution containing 0.1 mmol L^{-1} EP in B–R buffer (pH 7.4). This figure illustrates that it is possible to discriminate morphine from epinephrine with good separation in the peak potential (ΔE = +0.18 V).

4.2. Morphine, ascorbic acid and uric acid

Acute and chronic morphine administrations increase dopamine (DA) turnover[53] and release[54] in terminal fields of dopaminergic neurons. Increased dopaminergic activity in the limbic area and in the striatum is paralleled by increased locomotor activity and stereotyped behavior.[55] The dopaminergic system is also involved in the reinforcing effects of abused drugs.[56] Experimental evidence suggests that ascorbic acid (AA) may modulate central dopaminergic transmission[57] as well as behavior.[58] AA is not synthesized in the brain, and then diffuses at the blood–brain barrier site. AA is a very active component of the neuronal antioxidant pool, since it is rapidly oxidized by reactive oxygen species (ROS).[59] AA is the main scavenger of ROS generated from catecholamine oxidation *in vivo*.[60]

It is well known that large doses of AA have been reported to suppress withdrawal symptoms in opiate addicts and to prevent the development of tolerance and physical dependence on MO. Moreover, MO increases UA levels and AA oxidation. Therefore, the electrochemical behavior of MO in the presence of high concentrations of AA and UA is very crucial from the clinical point of view. DPV was used for the characterization of a solution containing a mixture of 5.0 mM AA, 1.0 mM UA and 0.5 mmol L^{-1} MO. Fig. 9A shows the determination of each one of the components of this mixture alone at [electrode (1)], which shows that the oxidation peak potential was at +410 mV for MO, +308 mV for UA, and +212 mV for AA. Broad peaks with weak responses were obtained when all the analytes were in the same mixture (Fig. 9B). This problem was solved by using [electrode (2)], where the anodic peak current of AA and UA disappears (Fig. 9C), which means that neither AA nor UA can interfere with MO when they are in a mixture in the case of using [electrode (2)]. Fig. 9D shows the voltammograms of MO, AA and UA mixture, under the optimum experimental conditions. As can be noticed in the case of [electrode (1)], only broad peaks occur for MO, UA and AA, while in the case of [electrode (2)] one sharp peak with the relatively higher oxidation peak current for MO was observed. These results prove that [electrode (2)] is more selective for MO even in the presence of high concentrations of AA and UA. The elimination of the interference effect of AA and UA was due to the negatively charged surface of

Table 3 Recovery data obtained by the standard addition method for MO in drug formulation

Formulation	[Tablet] taken $\times 10^{-5}$ mol L^{-1}	[Standard] added $\times 10^{-5}$ mol L^{-1}	Found $\times 10^{-6}$ mol L^{-1}	Recovery (%)	RSD (%)
Morphine sulfate	2.50	2.0	4.515	100.3	0.53
	8.00		10.04	100.4	0.43
	10.0		11.99	99.90	0.41
	20.0		22.02	100.1	0.17

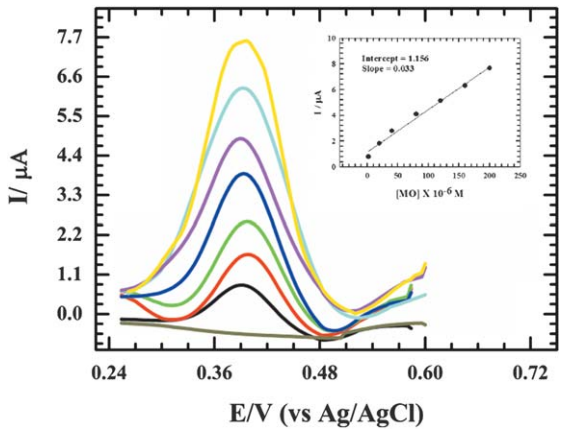

Fig. 10 Validation of the quantitative assay of the MO in urine using DPV in B–R buffer, pH 7.4, at a scan rate of 10 mV s^{-1}. The inset: the relation between MO concentrations in urine and the current responses.

[electrode (2)]. At the working pH of 7.4, MO was mainly in the protonated form which can be attracted to the electrode surface, while AA with a pK_a of 4.2[61] and UA with a pK_a of 5.4[61] were in their anionic forms and were repelled by the negatively charged gold particles.[62]

5. Analytical applications

5.1. Analysis of morphine sulfate® tablets

The determination of MO in its pharmaceutical formulation (10 mg per tablet) without the necessity for any extraction steps was performed. Five tablets of morphine sulfate were weighed and the average mass per tablet was determined, then these tablets were powdered. A portion of the fine powder was used to obtain a 1.0×10^{-3} mol L^{-1} solution. Aliquots of the drug solution were introduced into the electrolytic cell and the general procedure was carried out based on the average of three replicate measurements. The average standard MO concentration was taken as a base value. Then, known quantities of morphine sulfate tablets were added to the aliquot, and its concentrations were determined following the developed procedure. From Table 3 we can see that the recovery data obtained by the standard addition method for MO in drug formulation were found to be in the range from 99.9% to 100.4% and the relative standard deviation (RSD) was in the range from 0.17% to 0.53% suggesting that [electrode (2)] has higher reproducibility and that there were no important matrix interferences for the samples analyzed by the DPV mode and it would be a useful electrode for quantitative analysis of MO in pharmaceutical formulations.

5.2. Validation method in urine

Validation of the procedure for the quantitative assay of MO in urine was examined in B–R buffer, pH 7.4, at a scan rate of 10 mV s^{-1} using DPV (Fig. 10). The calibration curve (the inset) gave a straight line in the linear dynamic range of 2×10^{-6} mol L^{-1}–2×10^{-4} mol L^{-1} with the correlation coefficient $r = 0.9942$, the LOD is 8.72×10^{-8} mol L^{-1} and the LOQ is 2.90×10^{-7} mol L^{-1}. Four different concentrations on the calibration curve are chosen to be repeated for five times to evaluate the accuracy and precision of the proposed method which is represented in Table 4. Also the recovery, standard deviation, standard error and the confidence were calculated.

5.3. Robustness

The robustness was examined by evaluating the influence of small variation of some of the most important procedure variables. As it can be seen in Table S1§, the obtained results provided an indication of the reliability of the proposed procedure for the assay of MO and hence it can be considered robust. The obtained mean percentage recoveries based on the average of four replicate measurements were not significantly affected within the studied range of variations of some operational parameters, also the carbon paste electrode is stable with the advantage of the renewal of its surface without changing its properties and consequently the proposed procedure can be considered robust.

5.4. Ruggedness

Two analysts analyzed the same standard with two different instruments using the same method. The instruments were found

Table 4 Evaluation of the accuracy and precision of the proposed method for the determination of MO in urine sample

[MO] added $\times 10^{-5}$ mol L^{-1}	[MO] found[a] $\times 10^{-5}$ mol L^{-1}	Recovery (%)	SD $\times 10^{-6}$	SE[b] $\times 10^{-6}$	CL[c] $\times 10^{-6}$
5.00	5.018	100.30	0.47	0.19	0.37
10.0	9.990	99.900	0.35	0.15	0.46
14.0	14.01	100.07	0.20	0.090	0.65
22.0	21.97	99.800	0.55	0.25	0.68

[a] Mean for five determinations [b] Standard error = SD/$n^{1/2}$ [c] Confidence at 95% confidence level and 4 degrees of freedom (r=2.776)

to be rugged, with the results of variation coefficients of 0.37% and 0.62% (for AEW2 electrochemistry workstation) and 0.44% and 0.78% (for Bioanalytical systems, BAS,West Lafayette, USA) for the first and second analysts, respectively. The results show no statistical differences between analysts.

6. Conclusion

In the present work, we combine the advantages of Nafion (good ion-exchange and preconcentration features towards morphine molecules) and the high electrocatalytic activity of Au nanoparticles. A gold nanoparticle/carbon paste/Nafion system is used as a new and very efficient strategy to construct [electrode (2)]. The modified electrode has been shown to be efficient for the electrocatalytic oxidation of morphine. Furthermore it is very stable and efficient for the immobilization of MO at the surface of the modified electrode. The selective determination of MO in the presence of AA and UA in B–R buffer (pH 7.4) using [electrode (2)] was achieved with an excellent sensitivity.

The results showed that the method was simple and sensitive enough for determination of MO in clinical preparations (human urine) and in commercial tablets under physiological conditions with good precision, accuracy, selectivity and very low detection limit (picomolar). Compared with other methods for the assay of MO, [electrode (2)] sensor has good current response and the results are fairy satisfactory and beside that the background does not cause any significant effects.

Acknowledgements

The authors would like to express their gratitude to the University of Cairo (Office of Vice President for Graduate Studies and Research) for providing partial financial support through "The Young Researchers' Program." We would like to acknowledge the financial support by the National Organization for Drug Control and Research (NODCAR, Egypt).

References

1 C. P. Andrieux, P. Audebert, B. Divisia-Blohorn, P. Aldebert and F. Michalak, Electrochemistry in hydrophobic Nafion gels: part 2. Electrochemical behaviour and catalytic properties of electrodes modified by hydrophobic Nafion gels loaded with 9-phenylacridinium salts and anthraquinone, *J. Electroanal. Chem.*, 1990, **296**, 129–139.
2 D. Boyd, J. R. Barreira Rodriguez, A. J. Miranda Ordieres, P. Tunon Blanco and M. R. Smyth, Voltammetric study of salbutamol, fenoterol and metaproterenol at unmodified and Nafion-modified carbon-paste electrodes, *Analyst*, 1994, **119**, 1979–1984.
3 S. Moane, J. R. Barreira, M. Ordieres, P. Tuñon and M. R. Smyth, Electrochemical behaviour of clenbuterol at nation-modified carbon-paste electrodes, *J. Pharm. Biomed. Anal.*, 1995, **14**, 57–63.
4 H. Li, Y. Li, J. Li, E. Wang and S. Dong, Electroactive coatings of dicyano-bis(1,10-phenanthroline)iron(II) attached to Nafion polymer film modified electrodes *via* adsorption, *Electroanalysis*, 1995, **7**, 742–745.
5 J. Weber, L. Dunsch and A. Neudeck, Carbon fibre electrodes modified with Nafion®, *Electroanalysis*, 1995, **7**, 255–259.
6 S. Capelo, A. M. Mota and M. L. S. Goncalves, Complexation of lead with humic matter by stripping voltammetry. Prevention of adsorption on Nafion-coated mercury film electrode, *Electroanalysis*, 1995, **7**, 563–568.
7 B. Hoyer, T. M. Florence and G. E. Batley, Application of polymer-coated glassy carbon electrodes in anodic stripping voltammetry, *Anal. Chem.*, 1987, **59**, 1608–1614.
8 B. Hoyer and T. M. Florence, Application of polymer-coated glassy carbon electrodes to the direct determination of trace metals in body fluids by anodic stripping voltammetry, *Anal. Chem.*, 1987, **59**, 2839–2842.
9 H. Li, R. Ge and E. Wang, Catalytic oxidation and flow detection of acetaminophen at a dicyanobis(1,10-phenanthroline)iron(II)-modified electrode, *Anal. Chim. Acta*, 1994, **292**, 107–112.
10 D. Boyd, J. R. Barreira Rodriguez, P. Tuñon Blanco and M. R. Smyth, Application of a Nafion-modified carbon paste electrode for the adsorptive stripping voltammetric determination of fenoterol in pharmaceutical preparations and biological fluids, *J. Pharm. Biomed. Anal.*, 1994, **12**, 1069–1074.
11 C. R. Martin and H. Freiser, Ion-selective electrodes based on an ionic polymer, *Anal. Chem.*, 1981, **53**, 902–904.
12 M. N. Szentirmay and C. R. Martin, Ion-exchange selectivity of Nafion® films on electrode surfaces, *Anal. Chem.*, 1984, **56**, 1898–1902.
13 I. Rubinstein and A. J. Bard, Polymer films on electrodes. 5. Electrochemistry and chemiluminescence at Nafion®-coated electrodes, *J. Am. Chem. Soc.*, 1981, **103**, 5007–5013.
14 P. Ugo, B. Ballarin, S. Daniele and G. A. Mazzocchin, Electrochemistry of Yb^{3+} and Eu^{3+} at Nafion® modified electrodes, *J. Electroanal. Chem.*, 1990, **291**, 187–199.
15 P. Ugo, B. Ballarin, S. Daniele and G. A. Mazzocchin, Determination of trace amounts of Eu^{3+} and Yb^{3+} ions at Nafion-coated thin mercury film electrodes, *Anal. Chim. Acta*, 1991, **244**, 29–38.
16 J. Zhou and E. Wang, Ion exchange of cationic drugs at a Nafion-coated electrode in flow-through analysis, *Anal. Chim. Acta*, 1991, **249**, 489–494.
17 W. Huang, W. Qian, P. Jain and M. El-Sayed, The effect of plasmon field on the coherent lattice phonon oscillation in electron-beam nanofabricated gold particle pairs, *Nano Lett.*, 2007, **7**, 3227–3234.
18 O. P. Khatri, K. Murase and H. Sugimura, Structural organization of gold nanoparticles onto the ITO surface and its optical properties as a function of ensemble size, *Langmuir*, 2008, **24**, 3787–3793.
19 L. Guczi, G. Peto, A. Beck, K. Frey, O. Geszti, G. Molnar and C. Daroczi, Gold nanoparticles deposited on SiO_2/Si(100): correlation between size, electron structure and activity in CO oxidation, *J. Am. Chem. Soc.*, 2003, **125**, 4332–4337.
20 N. F. Atta, A. Galal, F. M. Abu-Attia and S. M. Azab, Carbon paste gold nanoparticles sensor for the selective determination of dopamine in buffered solution, *J. Electrochem. Soc.*, 2010, **157**, 116–123.
21 Z. F. Chen and Y. Zu, Selective detection of uric acid in the presence of ascorbic based on electrochemiluminescence quenching and highly enhanced activity, *Langmuir*, 2007, **23**, 11387–11390.
22 H. Qiu, G. Zhou, G. Ji, Y. Zhang, X. Huang and Y. Ding, A novel nanoporous gold modified electrode for the selective determination of dopamine in the presence of ascorbic acid, *Colloids Surf., B*, 2009, **69**, 105–108.
23 Y. Liu, X. Feng, J. Shen, J. Zhu and W. Hou, Fabrication of a novel glucose biosensor based on a highly electroactive polystyrene/polyaniline/Au nanocomposite, *J. Phys. Chem. B*, 2008, **112**, 9237–9242.
24 B. Fryirs, M. Dawson and L. E. Mather, Highly sensitive gas chromatographic-mass spectrometric method for morphine determination in plasma that is suitable for pharmacokinetic studies, *J. Chromatogr., Biomed. Appl.*, 1997, **693**, 51–57.
25 U. Hofmann, S. Seefried, E. Schweizer, T. Ebner, G. Mikus and M. Eichelbaum, Highly sensitive gas chromatographic-tandem mass spectrometric method for the determination of morphine and codeine in serum and urine in the femtomolar range, *J. Chromatogr., Biomed. Appl.*, 1999, **727**(1–2), 81–88.
26 P. P. Rop, F. Grimaldi, J. Burle, M. N. De saint leger and A. Viala, Determination of 6-monoacetylmorphine and morphine in plasma, whole blood and urine using high performance liquid chromatography with electrochemical detection, *J. Chromatogr., Biomed. Appl.*, 1994, **661**, 245–253.
27 S. R. Edwards and M. T. Smith, Simultaneous determination of morphine, oxycodone, morphine-3-glucouronide and noroxycodone concentrations in rat serum by high performance liquid chromatography-electrospray ionization tandem mass spectrometry, *J. Chromatogr., B: Anal. Technol. Biomed. Life Sci.*, 2005, **814**, 241–249.
28 M. Mabuchi, S. Takatsuka, M. Matsuoka and K. Tagawa, Determination of morphine, morphine-3-glucuronide and morphine-6-glucuronide in monkey and dog plasma by high-

performance liquid chromatography-electrospray ionization tandem mass spectrometry, *J. Pharm. Biomed. Anal.*, 2004, **35**, 563–573.
29 K. L. Crump, I. M. McIntyre and O. H. Drummer, Simultaneous determination of morphine and codeine in blood and bile using dual ultraviolet and fluorescence high performance liquid chromatography, *J. Anal. Toxicol.*, 1994, **18**, 208–212.
30 R. Aderjan, S. Hofmann, G. Schmitt and G. Skopp, Morphine and morphine glucuronides in serum of heroin consumers and in heroin-related deaths determined by HPLC with native fluorescence detection, *J. Anal. Toxicol.*, 1995, **19**, 163–168.
31 S. O. Mashayekhi, M. Ghandforoush-Sattari and R. D. W. Hain, Rapid and sensitive quantitation of morphine using HPLC with electrochemical detection, *Clin. Pharm. Ther.*, 2008, **33**, 419–427.
32 G. Sakai, K. Ogata, T. Uda, N. Miura and N. Yamazoe, A surface Plasmon resonance based immunosensor for highly sensitive detection of morphine, *Sens. Actuators, B*, 1998, **49**, 5–12.
33 N. Miura, K. Ogata, G. Sakai, T. Uda and N. Yamazoe, Detection of morphine in ppb range by using SPR (surface-plasmon-resonance) immunosensor, *Chem. Lett.*, 1997, 713–714.
34 D. J. Chapman, S. P. Joel and G. W. Aherne, Evaluation of a differential radioimmunoassay technique for the determination of morphine and morphine-6-glucuronide in human plasma, *J. Pharm. Biomed. Anal.*, 1994, **12**, 353–360.
35 N. F. Atta, A. Galal and R. A. Ahmed, Direct and simple electrochemical determination of morphine at PEDOT modified Pt electrode, *Electroanalysis*, 2011, **23**, 737–746.
36 B. Proksa and L. Molar, Voltammetric determination of morphine on stationary platinum and graphite electrodes, *Anal. Chim. Acta*, 1978, **97**, 149–154.
37 A. Niazi and A. Yazdanipour, Spectrophotometric simultaneous determination of nitrophenol isomers by orthogonal signal correction and partial least squares, *Chin. Chem. Lett.*, 2007, **146**, 421–427.
38 A. Niazi, J. Ghasemi and M. Zendehdel, Simultaneous voltammetric determination of morphine and noscapine by adsorptive differential pulse stripping method and least-squares support vector machines, *Talanta*, 2007, **74**, 247–254.
39 P. Norouzi, M. R. Ganjali, A. A. Moosavi-movahedi and B. Larijani, Fast Fourier transformation with continuous cyclic voltammetry at an Au microelectrode for the determination of morphine in a flow injection system, *Talanta*, 2007, **73**, 54–61.
40 M. R. Ganjali, P. Norouzi, R. Dinarvand, R. Farrokhi and A. A. Moosavi-movahedi, Development of fast Fourier transformations with continuous cyclic voltammetry at an Au microelectrode and its application for the sub nano-molar monitoring of methyl morphine trace amounts, *Mater. Sci. Eng., C*, 2008, **28**, 1311–1318.
41 F. Xu, M. N. Gao, L. Wang, T. S. Zhou, L. T. Jin and J. Y. Jin, Amperometric determination of morphine on cobalt hexacyanoferrate modified electrode in rat brain microdialysates, *Talanta*, 2002, **58**, 427–432.
42 K. C. Ho, C. Y. Chen, H. C. Hsu, L. C. Chen, S. C. Shiesh and X. Z. Lin, Amperometric detection of morphine at a Prussian blue-modified indium tin oxide electrode, *Biosens. Bioelectron.*, 2004, **20**, 3–8.
43 W. M. Yeh and K. C. Ho, Amperometric morphine sensing using a molecularly imprinted polymer-modified electrode, *Anal. Chim. Acta*, 2005, **542**, 76–82.
44 K. C. Ho, W. M. Yeh, T. S. Tung and J. Y. Liao, Amperometric detection of morphine based on poly(3,4-ethylenedioxythiophene) immobilized molecularly imprinted polymer particles prepared by precipitation polymerization, *Anal. Chim. Acta*, 2005, **542**, 90–96.
45 A. Salimi, R. Hallaj and G. R. Khayatian, Amperometric detection of morphine at preheated glassy carbon electrode modified with multiwall carbon nanotubes, *Electroanalysis*, 2005, **17**, 873–879.
46 M. H. Pournaghi-Azar and A. Saadatirad, Simultaneous voltammetric and amperometric determination of morphine and codeine using a chemically modified palladized aluminum electrode, *J. Electroanal. Chem.*, 2008, **624**, 293–298.
47 S. Shahrokhian and M. Ghalkhani, Simultaneous voltammetric detection of ascorbic acid and uric acid at a carbon-paste modified electrode incorporating thionine–nafion ion-pair as an electron mediator, *Electrochim. Acta*, 2006, **51**, 2599–2606.
48 J. M. P. J. Garrido, C. D. Matos, F. Borges, T. R. A. Macedo and A. M. O. Brett, Voltammetric oxidation of drugs of abuse. I. morphine and metabolites, *Electroanalysis*, 2004, **16**, 1419–1426.
49 S. D. Roy and G. L. Flynn, Transdermal delivery of narcotic analgesics: comparative permeabilities of narcotic analgesics through human cadaver skin, *Pharm. Res.*, 1989, **6**, 825–832.
50 N. Yang, Q. Wan and J. Yu, Adsorptive voltammetry of Hg(II) ions at a glassy carbon electrode coated with electropolymerized methyl-red film, *Sens. Actuators, B*, 2005, **110**, 246–251.
51 W. Qijin, Y. Nianjun, Z. Haili, Z. Xinpin and X. Bin, Voltammetric behavior of vitamin B_2 on the gold electrode modified with a self-assembled monolayer of L-cysteine and its application for the determination of vitamin B_2 using linear sweep stripping voltammetry, *Talanta*, 2001, **55**, 459–467.
52 N. F. Atta, A. Galal, F. M. Abu-Attia and S. M. Azab., Characterization and electrochemical investigations of micellar/drug interactions, *Electrochim. Acta*, 2010, **56**, 2510–2517.
53 L. Ahtee, L. M. J. Attila, K. R. Carlson and H. Haikala, Changes in brain monoamine metabolism during withdrawal from chronic oral self-administration of morphine and in response to a morphine challenge in the withdrawn state, *J. Pharmacol. Exp. Ther.*, 1989, **249**, 303–310.
54 G. D. Chiara and A. Imperato, Opposite effects of mu and kappa opiate agonists on dopamine release in the nucleus accumbens and in the dorsal caudate of freely moving rats, *J. Pharmacol. Exp. Ther.*, 1988, **244**, 1067–1080.
55 G. K. Aghajanian, J. H. Kogan and B. Moghaddam, Opiate withdrawal increases glutamate and aspartate efflux in the locus coeruleus: an in vivo microdialysis study, *Brain Res.*, 1994, **6336**, 126–130.
56 E. Acquas and G. D. Chiara, Depression of mesolimbic dopamine transmission and sensitization to morphine during opiate abstinence, *J. Neurochem.*, 1992, **58**, 1620–1625.
57 G. V. Rebec and C. P. Pierce, A vitamin as neuromodulator: ascorbate release into the extracellular fluid of the brain regulates dopaminergic and glutamatergic transmission, *Prog. Neurobiol.*, 1994, **43**, 537–565.
58 L. D. Angeli, Ascorbic acid and atypical antipsychotic drugs: modulation of aminopeptine-induced behavior in mice, *Brain Res.*, 1995, **670**, 303–307.
59 G. Paxinos and C. Watson, The Rat Brain in *Stereotaxic Coordinates*, Academic Press, New York, 1982.
60 V. A. Roginsky, T. K. Barsukova, G. Bruchelt and H. B. Stegmann, Interaction of catecholamines and 6-hydroxy-dopamine with ascorbate during autoxidation, *Pharmacol. Res.*, 1995, **31**, 141.
61 J. Li and X.-Q. Lin, Electrodeposition of gold nanoclusters on overoxidized polypyrrole film modified glassy carbon electrode and its application for the simultaneous determination of epinephrine and uric acid under coexistence of ascorbic acid, *Anal. Chim. Acta*, 2007, **596**, 222–230.
62 Z. Nasri and E. Shams, Application of silica gel as an effective modifier for the voltammetric determination of dopamine in the presence of ascorbic acid and uric acid, *Electrochim. Acta*, 2009, **54**, 7416–7421.